Pulse Radiolytic Kinetic Study of the Decay of α-Methyl-Substituted Benzoquinone Radical Anions: A Possible Mechanistic Model for Bioreductive Alkylation

Kevin E. O'Shea and Marye Anne Fox*

Contribution from the Department of Chemistry, University of Texas, Austin, Texas 78712.
Received July 24, 1990

Abstract: Pulse radiolysis and transient absorption spectroscopy were used to kinetically characterize the decay of several α-methyl-substituted 1,4-benzoquinone radical anions. Electron attachment rates, absorption spectra, extinction coefficients, and pK_a's for the reduced quinones are very similar regardless of substituent, but the decay kinetics are dependent on both substituent and pH. The semiquinone radical anions disproportionate at pH 7 regardless of substituent. At pH 3, the radical anion is readily protonated, and in the phenoxy- and methoxy-substituted models reductive elimination becomes competitive with disproportionation. The involvement of an intramolecular H-bonded intermediate is proposed in the formation of the quinone methide. The existence of such an intermediate is supported by theoretical results (AM1 calculations).

Introduction

Bioreductive alkylation,[1-3] a term that describes a mode of biological action initiated by in vivo reduction of a latent alkylating agent, is especially useful in the development of antineoplastic agents. Quinones commonly function as the reducible moiety of these agents because of their facile in vivo and in vitro reduction. Selective activation of quinoid antibiotic antitumor drugs (e.g., mitomycins, saframycins, and anthracyclines) is possible in tumor tissues because of their greater capacity for reduction over normal oxygenated cells.[3-6] Upon enzymatic reduction, the quinone moiety forms a semiquinone radical anion, which may transfer an electron, disproportionate, or form a quinone methide by loss of an anionic leaving group originally bound β (or an appropriate vinylogous position) to the carbonyl, Scheme I. A good leaving group at the β-position should facilitate quinone methide formation by faciliating reductive cleavage.[1,2] The resulting α,β-unsaturated enone is thus strongly activated toward nucleophilic attack (e.g., by nucleophilic bases of DNA). Determining the role of these intermediates is key to the design and development of effective bioreductive alkylating drugs.

Although numerous studies have implicated the quinone methide as the key intermediate responsible for biological activity,[7-19] the mechanism leading to its formation is not clearly or completely understood. Sartorelli and co-workers have shown that compounds designed to give facile quinone methide formation show enhanced biological activity,[1,3] but little kinetic information is available concerning C–X bond cleavage in the singly or doubly reduced quinone, particularly in comparison with rates of disproportionation of the radical anion.[20]

Scheme I. General Mechanism Proposed for Bioreductive Alkylation[2]

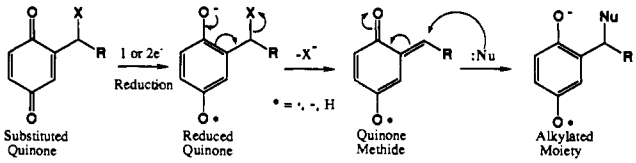

In this study, transient absorption spectroscopy was used to characterize the one-electron-reduced form of these models, generated by pulse radiolytic electron attachment,[21] and to kinetically analyze its subsequent chemistry. The effect of pH was studied in order to determine its influence on the kinetics and to elucidate the possible role of the protonated forms of the reduced species. From these studies, we define the role of the semiquinone radical anion, semiquinone radical, hydroquinone, and quinone methide as possible intermediates in the proposed activation cascade.[10,13,15] The intervention of an intramolecularly H-bonded intermediate to facilitate formation of the quinone methide in models bearing leaving groups capable of hydrogen bonding is proposed. Calculations suggest that this intermediate is stabilized in comparison with the analogous non-hydrogen-bonded intermediate. Product studies were not undertaken because of limited solubilities of these models in water, the difficulties associated with scale-up of pulse radiolytic experiments, and the infeasibility

(1) (a) Lin, A. J.; Cosby, L. A.; Shansky, C. W.; Sartorelli, A. C. *J. Med. Chem.* **1972**, *15*, 1247. (b) Lin, A. J.; Sartorelli, A. C. *J. Org. Chem.* **1973**, *38*, 813. (c) Lin, A. J.; Pardini, R. S.; Cosby, L. A.; Lillis, B. J.; Shansky, C. W.; Sartorelli, A. C. *J. Med. Chem.* **1973**, *16*, 1268. (d) Lin, A. J.; Shansky, C. W.; Sartorelli, A. C. *J. Med. Chem.* **1974**, *17*, 558. (e) Lin, A. J.; Lillis, B. J.; Sartorelli, A. C. *J. Med. Chem.* **1975**, *18*, 917. (f) Lin, A. J.; Sartorelli, A. C. *J. Med. Chem.* **1976**, *19*, 1336. (g) Lin, T.-S.; Teicher, B. A.; Sartorelli, A. C. *J. Med. Chem.* **1980**, *23*, 1237. (h) Wilson, I.; Wardman, P.; Lin, T.-S.; Sartorelli, A. C. *J. Med. Chem.* **1986**, *29*, 1381.

(2) (a) Moore, H. W. *Science* **1977**, *197*, 527. (b) Moore, H. W.; Czerniak, R.; Hamdan, A. *Drugs Exp. Clin. Res.* **1986**, *12* (6/7), 475.

(3) Lin, A. J.; Sartorelli, A. C. *Biochem. Pharmacol.* **1976**, *25*, 206.

(4) Cater, D. B.; Phillips, A. F. *Nature* **1954**, *174*, 121.

(5) Prakash, G.; Hodnett, E. M. *J. Med. Chem.* **1978**, *21*, 369.

(6) (a) Rao, G. M.; Lown, J. W.; Plambeck, J. A. *J. Electrochem. Soc.* **1977**, *124*, 195. (b) Rao, G. M.; Begleiter, A.; Lown, J. W.; Plambeck, J. A. *J. Electrochem. Soc.* **1977**, *124*, 199.

(7) Iyer, V. N.; Szybalski, W. *Science* **1964**, *145*, 55.

(8) Szmigiero, L.; Erickson, L. C.; Ewig, R. A.; Kohn, K. W. *Cancer Res.* **1984**, *44*, 4447.

(9) (a) Land, E. J. *J. Chem. Soc., Faraday Trans. 2* **1986**, *82*, 2183. (b) Land, E. J.; Mukherjee, T.; Swallow, A. J.; Bruce, J. M. *Br. J. Cancer* **1985**, *51*, 515.

(10) Danishefsky, S. J.; Egbertson, M. *J. Am. Chem. Soc.* **1986**, *108*, 4648.

(11) Gutierrez, P. L.; Biswal, S.; Nardino, R.; Biswal, N. *Cancer Res.* **1986**, *46*, 5779.

(12) (a) Kohn, H.; Zein, N.; Lin, X. Q.; Ding, J.-Q.; Kadish, K. M. *J. Am. Chem. Soc.* **1987**, *109*, 1833. (b) Zein, N.; Kohn, H. *J. Am. Chem. Soc.* **1987**, *109*, 1576.

(13) (a) Tomasz, M.; Lipman, R.; Chowdray, D.; Pawlak, J.; Verdine, G. L.; Nakanishi, K. *Science* **1987**, *235*, 1204. (b) Tomasz, M.; Lipman, R.; Verdine, G. L.; Nakanishi, K. *J. Am. Chem. Soc.* **1985**, *107*, 6120.

(14) Butler, J.; Hoey, B. M.; Ward, T. H. *Biochem. Pharmacol.* **1989**, *38*, 923.

(15) (a) Boldt, M.; Gaudiano, G.; Haddadin, M. J.; Koch, T. H. *J. Am. Chem. Soc.* **1989**, *111*, 2283. (b) Egholm, M.; Koch, T. H. *J. Am. Chem. Soc.* **1989**, *111*, 8291.

(16) (a) Favandon, V. *Biochemie* **1982**, *64*, 457. (b) Svingen, B. A.; Powis, G. *Arch. Biochem. Biophys.* **1981**, *209*, 119. (c) Bachur, N. R.; Gordon, S. L.; Gee, M. V. *Cancer Res.* **1978**, *38*, 1745.

(17) Kavabelas, K.; Moore, H. W. *J. Am. Chem. Soc.* **1990**, *112*, 5372.

(18) (a) Kinoshita, S.; Uzu, K.; Nakano, K.; Takahashi, T. *J. Med. Chem.* **1971**, *14*, 109. (b) Kinoshita, S.; Uzu, K.; Nakano, K.; Shimizu, M.; Takahashi, T. *J. Med. Chem.* **1971**, *14*, 103.

(19) Lown, J. W. *Acc. Chem. Res.* **1982**, *15*, 381.

(20) Swallow, J. A.; Ross, A. B.; Helman, W. P. *Radiat. Phys. Chem.* **1981**, *17*, 127.

(21) (a) Neta, P. In *The Chemistry of Quinonoid Compounds*; Patai, S., Rappoport, Z., Eds.; Wiley: New York, 1986; Vol. II, Chapter 14. (b) Buxton, G. V. In *The Study of Fast and Transient Species by Electron Pulse Radiolysis*; Baxendale, J. H., Busi, F., Eds.; Reidel, D.: Dordrecht, 1982. (c) Buxton, G. V. In *Radiation Chemistry Principles and Applications*; Farhataziz, Rodgers, M. A. J., Eds.; VCH Publishers: New York, 1987; p 332.

0002-7863/91/1513-611$02.50/0

of directly comparing products obtained under more propitious reducing conditions (e.g., by alkali metals in nonaqueous solvents) with those deriving specifically from the radical anions in these experiments.

Experimental Section

Materials. 1,4-Benzoquinone (recrystallized from hexanes), 2-methyl-1,4-benzoquinone (recrystallized from hexanes), phenoxyacetic acid, methoxyacetic acid, silver nitrate, and 2,5-dimethoxybenzyl alcohol were purchased from Aldrich Chemical Co. *N*-Bromosuccinimide (NBS) (MCB Chemicals) was purified by recrystallization from water. Ceric ammonium nitrate (G. Fredrick Smith), triphenylphosphine (Lancaster Synthesis), *tert*-butyl alcohol (J. T. Baker), and the potassium phosphate (Fisher Scientific) were used as received.

Instrumentation. Melting points were determined in a Mel-Temp instrument and are uncorrected. Flash column chromatography was performed on Merck Kieselgel 60 silica (230–400 mesh). Gas–liquid chromatographic (GC) analyses were conducted on a Hewlett-Packard 5890A instrument equipped with a 25-m DB-5 capillary column and a flame ionization detector. Mass spectrometry was performed on a Finnigan 4023 automated GC/MS equipped with a 25-m DB-1 capillary column. UV spectra were measured as aqueous solutions on a Hewlett-Packard 845A diode array spectrophotometer. Proton and carbon nuclear magnetic resonance spectra, obtained on a General Electric QE300 spectrometer, are reported in parts per million relative to $(CH_3)_4Si$ or $CDCl_3$ as internal standards.

Calculations. Calculations of spin distributions, formal charges, bond lengths and angles, geometries, and heats of formation were carried out with use of standard AM1[22] (UHF[23]) procedure as implemented in the AMPAC computer program.

Electron Accelerator. Pulse radiolysis experiments were performed on a previously described apparatus.[24] A 4-MeV (1–3 A) van de Graff accelerator was used to produce 2–20-Gy electron pulses (50, 100, 250, and 500 ns), which were delivered to the samples contained in a quartz flow cell with a 2.2 cm analyzing path length. Potassium phosphate buffer solutions were prepared with Millipore-filtered water. Solution pH was adjusted with dilute potassium hydroxide or sulfuric acid. *tert*-Butyl alcohol was added to scavenge hydroxide formed during irradiation. The solutions were bubbled with argon or nitrogen before each experiment. Fresh sample solution was injected into the cell after each pulse. The absorption of the solvated electron in water was used as a dosimeter.[21c]

2-(Bromomethyl)-1,4-benzoquinone (1). A solution of 2-methyl-1,4-benzoquinone (1.00 g, 8.2 mmol) and NBS (1.30 g, 9.1 mmol) in 50 mL of dry CH_2Cl_2 (freshly distilled over CaH_2) was stirred under N_2 while being irradiated by a 150-W sunlamp placed 6 in. from the reaction vessel. The solvent was evaporated at a reduced pressure, the resulting residue was taken up in CCl_4, and the undissolved solids, including succinimide, were filtered away. The product was purified by use of flash column chromatography, giving a dark red solid (60%): mp 61–62 °C; ^1H NMR ($CDCl_3$, 300 MHz) 6.86–6.75 (m, 3 H), 4.25 (s, 2 H) ppm; ^{13}C NMR ($CDCl_3$, 75 MHz) 186.9, 184.9, 144.1, 136.7, 136.4, 134.3, 24.5 ppm; HR-MS, *m/z* 199.9475 (M^+, calcd for $C_7H_5O_2{}^{79}Br$, 199.9473); UV (water) 252 (19 000), 320 (sh, 800) nm.

2-(Chloromethyl)-1,4-dimethoxybenzene. A solution of 2,5-dimethoxybenzyl alcohol (0.84 g, 5.0 mmol) and triphenylphosphine (1.68 g, 6.0 mmol) in 25 mL of CCl_4 was heated to reflux and stirred continuously under a positive pressure of nitrogen. After 12 h, the reaction mixture was washed with water. The organic phase was dried over $MgSO_4$ and the crude product purified by flash column chromatography. White solid (90% yield): mp 68–70 °C (lit.[25] mp 66–67 °C); ^1H NMR ($CDCl_3$, 300 MHz) 6.92–6.91 (m, 1 H), 6.81–6.84 (m, 2 H), 4.63 (s, 2 H), 3.85 (s, 3 H), 3.77 (s, 3 H) ppm; ^{13}C NMR ($CDCl_3$, 75 MHz) 153.5, 151.5, 126.7, 116.2, 114.7, 112.0, 56.2, 55.8, 41.5 ppm; MS, *m/z* 186, 171, 151, 137, 121, 91, 77, 65, 51, 39.

2-(Chloromethyl)-1,4-benzoquinone (2). To a solution of 2,5-dimethoxybenzyl chloride (0.167 g, 0.9 mmol) in 5 mL of CH_3CN was added dropwise an aqueous ceric ammonium nitrate (1.1 g, 2.0 mmol) solution. After the addition was complete, the reaction was stirred at room temperature (25 °C) for 30 min. The resulting solution was extracted with chloroform. The organic phase was washed with saturated NaCl solution and dried over $MgSO_4$. Removal of the solvent furnished a dark residue. The product was purified by flash column chromatography in 60% yield as a yellow solid: mp 43–45 °C; ^1H NMR ($CDCl_3$, 300 MHz) 6.92–6.91 (m, 1 H), 6.79–6.76 (m, 2 H), 4.39 (s, 2 H) ppm; ^{13}C NMR ($CDCl_3$, 75 MHz) 187.0, 185.6, 143.8, 136.8, 136.4, 133.7, 39.2 ppm; HR-MS, *m/z* 155.9986 (M^+, calcd for $C_7H_5O_2{}^{35}Cl$, 155.9978); UV (water) 252 (20 000), 310 (sh, 500) nm.

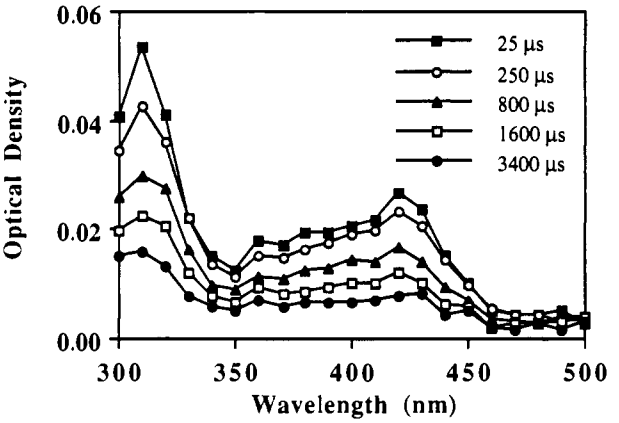

Figure 1. Transient absorption spectrum observed upon electron attachment to 2-(bromomethyl)-1,4-benzoquinone (2.4×10^{-4} M) in N_2-saturated 5 mM aqueous phosphate buffer solution at pH 7 containing 0.2 M *tert*-butyl alcohol; dose = 3 Gy/pulse. The spectrum is assigned to the semiquinone radical anion.

2-(Phenoxymethyl)-1,4-benzoquinone (3). The product was prepared by the method of Jacobsen and Torssell[26] and recrystallized from 95% ethanol to give yellow needles in 82% yield: mp 144–145 °C (lit.[26] mp 138–140 °C); ^{13}C NMR ($CDCl_3$, 75 MHz) 188.0, 187.3, 158.8, 145.1, 137.4, 137.3, 131.9, 130.4, 122.2, 115,5, 63.9 ppm; MS, *m/z* 214, 197, 185, 131, 118, 93, 77, 65, 51, 39; UV (water) 252 (19 000), 310 (sh, 1800) nm.

2-(Methoxymethyl)-1,4-benzoquinone (4). The product was prepared in parallel with **3**,[26] purified by column chromtography, and isolated as a rust-colored solid in 19% yield: mp 38–40 °C (lit.[26] mp 38–40 °C); ^{13}C NMR ($CDCl_3$, 75 MHz) 187.3, 186.8, 145.3, 136.4, 136.3, 131.1, 67.5, 59.0 ppm; MS, *m/z* 152, 137, 124, 109, 94, 81, 53, 39; UV (water) 250 (21 000), 310 (sh, 600) nm.

Results

Pulse Radiolysis of the Models in Aqueous Solutions. The primary products formed by irradiation of water with high-energy electrons are represented, eq 1.[21b,c] H_2O_2, H_3O^+, OH^-, and H_2

$$H_2O \rightsquigarrow e^-_{aq}, H^\bullet, OH^\bullet, H_2, H_2O_2, H_3O^+, OH^- \qquad (1)$$

are relatively stable, but e^-, $H^\bullet$, and $OH^\bullet$ are very reactive toward organic compounds, forming organic free radicals. To ensure that electrons are the predominant species reacting with the organic substrate, all solutions were purged with argon or nitrogen to eliminate oxygen and contained 0.2 M *tert*-butyl alcohol to scavenge hydroxyl radicals. The pH was kept between 3 and 7 in order to minimize the small primary yield of $H^\bullet$.[21c] We also note that since tumor cells are, on the average, more acidic than normal cells, differential cytotoxicity could best be probed in an acidic environment.[27]

The desired pathway involves initial attachment of an electron to generate the radical anion, eq 2. Transient absorption spectroscopy was used to measure the pK_a's, extinction coefficients,

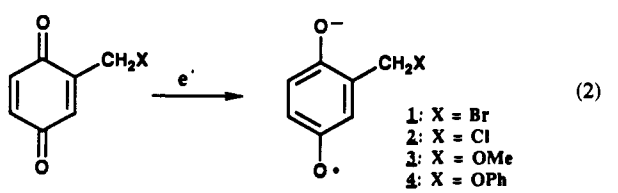

1: X = Br
2: X = Cl
3: X = OMe
4: X = OPh

(2)

(22) (a) Dewar, M. J. S.; Zoebisch, E. G.; Healy, E. F.; Stewart, J. J. P. *J. Am. Chem. Soc.* **1985**, *107*, 3902. (b) Available from the Quantum Chemistry Program Exchange, QCPE No. 506, Department of Chemistry, Indiana University, Bloomington, IN 47405.

(23) Pople, J. A.; Nesbet, R. K. *J. Chem. Phys.* **1954**, *22*, 571.

(24) Rodgers, M. A. J.; Foyt, D. C.; Zimek, Z. A. *Radiat. Res.* **1977**, *75*, 296.

(25) Kost, A. N.; Sagitullin, R. S.; Yurovskaya, M. A. *Zh. Obshch. Khim.* **1963**, *33*, 2011.

(26) Jacobsen, N.; Torssell, K. *Liebigs Ann. Chem.* **1972**, *763*, 135.

(27) (a) Tannock, I. F.; Rotin, D. *Cancer Res.* **1989**, *49*, 4373. (b) Vaupel, P.; Kallinowski, F.; Okunieff, P. *Cancer Res.* **1989**, *49*, 6449.

electron attachment rates, and decay kinetics for the semiquinone radical anions.

Transient Absorption Spectra. The transient absorption spectrum observed following electron attachment to 2-(bromomethyl)-1,4-benzoquinone (2.4×10^{-4} M), eq 1, in N_2-saturated 5 mM phosphate buffer solution at pH 7 containing 0.2 M *tert*-butyl alcohol is shown in Figure 1. This spectrum shows absorbance maxima at 310 and 420 nm that decay over 10 ms. Analogous experiments at pH 3 gave slightly blue-shifted spectra, with absorbance maxima at 300 and 400 nm. These spectra are similar to those reported for simple benzoquinones[28-31] and have been assigned to the semiquinone radical anion and its protonated form, the semiquonone radical, at pH 7 and 2, respectively.

The initial optical density at 430 nm (OD^0_{430}) for the transient formed at pH 7 is almost 10 times that observed at pH 3, Figure 2. In order to determine the pK of the radical anion,[32] the OD^0_{430} was measured as a function of pH.

$$Q^{\cdot-} + H^+ \rightleftharpoons QH^{\cdot}$$

A titration curve for reduced 2-(bromomethyl)-1,4-benzoquinone semiquinone radical anion, Figure 3, reveals an inflection point representative of the pK_a of the transient. The β-substituents do not drastically affect either the spectra or pK_a's of the reduced models, Table I, which all have lifetimes significantly longer than the width of the electron pulse (50–500 ns) and are readily protonated at low pH.

Extinction Coefficients. The extinction coefficients,[33] ϵ_λ, were calculated by dividing the optical densities of the transients extrapolated to time zero, OD^0_λ, by the product of the path length, l (cm), and concentration of transient, $[S^{\cdot-}]$, eqs 3 and 4. Here,

$$\epsilon_\lambda = OD^0_\lambda / [S^{\cdot-}]l \quad (3)$$

$$[S^{\cdot-}] = [e^-]f_s \quad (4)$$

the transient concentration, eq 4, is given by the product of f_s, the fraction of electrons scavenged by the substrate, and $[e^-]$, the concentration of electrons as determined from dosimetry.[21c] The shorter wavelength absorption bands are almost twice as intense as the longer wavelength bands at each pH. The methoxy- and phenoxy-substituted models absorb more strongly than the corresponding bromide and chloride, Table I.

Electron-Attachment Rates. The electron-attachment rates, k_e, were obtained by plotting the rate constants for the formation of the transient species as a function of solute concentration.[34] The growth of the transient species at its absorption maxima, Figure 4, was fit to first-order kinetics at several initial concentrations varying from 10^{-4} to 10^{-6} M. The plot of the observed rate constant, k_{obs}, against substrate concentration gives a straight line with the slope, representing the electron-attachment rate. Attachment rates at pH 7 obtained at each of the absorbance maxima, Table II, were identical.

Decay Kinetics. The data analysis system has been described in detail elsewhere.[35] The semiquinone radical anions decay via second-order kinetics at pH 7, Figure 5, where $k_{obs} = 2k_{decay}/\epsilon l$. The rate constants at each maxima are identical (within experimental error) and are independent of dose and concentration. The transient half-life decreases with increasing dose in accordance with second-order kinetics. This is assigned to disproportionation of the semiquinone radical anion to give half-equivalents of the quinone and the hydroquinone dianion, eq 5.

$$2Q^{\cdot-} \rightleftharpoons Q + Q^{2-} \quad (5)$$

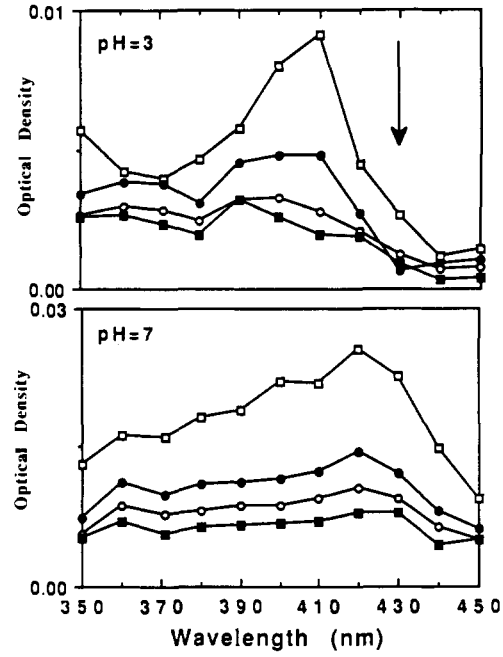

Figure 2. Transient absorption spectra at pH 3 and 7 after irradiation of 1.0×10^{-4} M aqueous 2-(bromomethyl)-1,4-benzoquinone in N_2-saturated 5 mM phosphate buffer solution with 0.2 M *tert*-butyl alcohol. The spectrum at pH 3 is assigned to the semiquinone radical, while that at pH 7 is attributed to the semiquinone radical anion.

Table I. Acidity, Absorption Maxima, and Extinction Coefficients for the Substituted Semiquinones

		λ_{max}[b] (nm) (ϵ[c] (M^{-1} cm^{-1}))	
quinone	pK_a[a]	pH 7	pH 3
1	4.1	310 (5400), 420 (3600)	300 (4400), 410 (3400)
2	4.0	310 (8300), 430 (4200)	300 (5900), 410 (3700)
3	3.8	310 (18 000), 420 (7600)	300 (7600), 400 (3600)
4	3.9	310 (13 500), 420 (6100)	300 (7100). 400 (4800)

[a] Accurate to within 0.5 pK unit. [b] Spectral intervals were monitored in the pulse experiments at 10-nm intervals. [c] Average of three or more determinations; 10–20% error based on standard deviation.

Table II. Electron Attachment Rates, k_e, for Formation of Semiquinone Radical Anions and Their Second-Order Decay Rates, k_d, at pH 7

	$k_e \times 10^{-9}$[a] (M^{-1} s^{-1})		$k_d \times 10^{-8}$[a,b] (M^{-1} s^{-1})	
quinone	320 nm	420 nm	310 nm	420 nm
1	1.3 (0.3)	1.7 (0.5)	1.4 (0.2)	1.2 (0.3)
2	1.4 (0.2)	1.6 (0.3)	1.8 (0.6)	1.6 (0.8)
3	2.1 (0.3)	2.1 (0.4)	1.1 (0.2)	0.7 (0.5)
4	1.5 (0.4)	*c*	5.4 (0.1)	5.0 (1.6)

[a] An average of two or more determinations; standard deviation in parentheses. [b] Errors were calculated from standard deviations of the extinction coefficients and observed rate constants. [c] The limited solutility and small extinction coefficient of the radical anion made access to the range of concentrations necessary for an accurate determination impossible.

Table III. Decay Rate Constants for the Semiquinone Radicals Formed at pH 3

		$k_{1st\ order}$[a] (10^{-3} s^{-1})		$k_{2nd\ order}$[a,b] (10^{-8} M^{-1} s^{-1})	
quinone	charactizn	300 nm	400 nm	300 nm	400 nm
1	2nd order			2.4 (0.7)	2.2 (0.3)
2	2nd order			7.4 (1.9)	4.4 (2.3)
3	competing 1st and 2nd order	1.0 (0.1)	0.8 (0.2)	5.5 (3.0)	2.5 (1.3)
4	competing 1st and 2nd order	4.4 (0.1)	4.1 (1.5)	2.8 (0.5)	3.2 (1.6)

[a] Average of three determinations. Uncertainty reported is the standard deviation. [b] Errors were calculated from standard deviations of the extinction coefficients and the observed rate constants.

(28) Land, E. J.; Porter, G. *Proc. Chem. Soc., London* **1960**, 84.
(29) Willson, R. L. *J. Chem. Soc., Chem. Commun.* **1971**, 1249.
(30) Patel, K. B.; Willson, R. L. *J. Chem. Soc., Faraday Trans. 1* **1973**, *69*, 814.
(31) Rao, P. S.; Hayon, E. *J. Phys. Chem.* **1973**, *77*, 2274.
(32) (a) Bridge, N. K.; Porter, G. *Proc. Roy. Soc., London* **1958**, *A244*, 276. (b) Adams, G. E.; Michael, B. D. *Trans. Faraday Soc.* **1967**, *63*, 1171.
(33) The solute concentrations were chosen to ensure 90–100% capture of electrons, but the limited solubility of 2-phenoxy-1,4-benzoquinone made a correction for its scavenging efficency necessary.
(34) Willson, R. L. *J. Chem. Soc., Faraday Trans. 1* **1971**, *67*, 3020.
(35) Foyt, D. C. *Comput. Chem.* **1981**, *5*, 49.

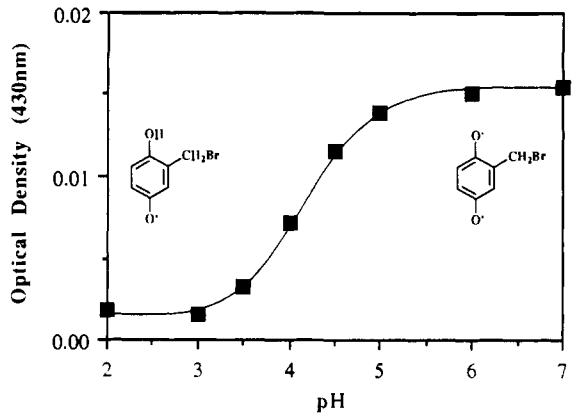

Figure 3. Acid dissociation constant (pK_a) curve for the semiquinone radical of 2-(bromomethyl)-1,4-benzoquinone. The optical density at 430 nm plotted as a function of pH. pK(semiquinone) = 4.1 (±0.5).

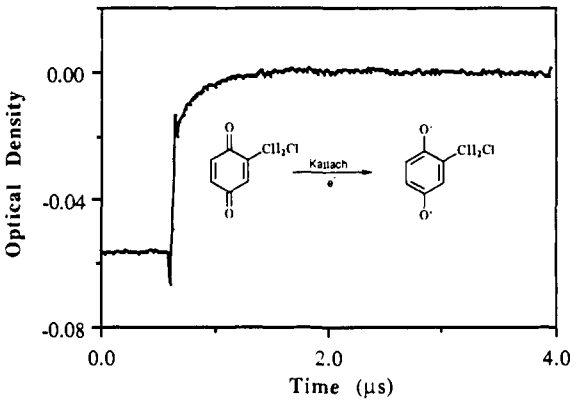

Figure 4. Growth of semiquinone radical anion transient (310 nm) from irradiation of 1.2×10^{-4} M 2-(chloromethyl)-1,4-benzoquinone in N_2-saturated 5 mM phosphate buffer at pH 7 containing 0.2 M *tert*-butyl alcohol (dose = 3 Gy/pulse).

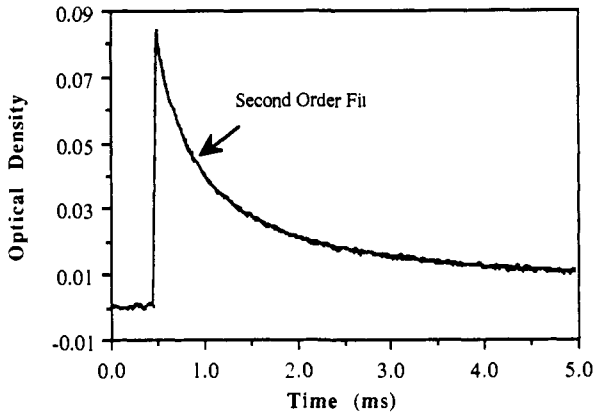

Figure 5. Transient decay observed (310 nm) following electron attachment to 2-(chloromethyl)-1,4-benzoquinone (1.1×10^{-4} M) in N_2-saturated neutral aqueous solution (dose = 6 Gy/pulse). Solid line represents a second-order fit.

The predominant transient species at pH 3 is the semiquinone radical formed from protonation of the radical anion. While the transients from the bromo and chloro derivatives decay by a second-order process, the methoxy- and phenoxy-substituted transients follow competing first- and second-order kinetics. The second-order rate constants for disproportionation of the bromide and chloride are faster than for the analogous reactions at pH 7, as is expected since neutral species can diffuse together more readily than can the negatively charged radical anions. A typical decay trace of the transient species formed from the radiolysis of 2-(methoxymethyl)-1,4-benzoquinone at pH 3 is shown in Figure 6. Although the second-order decay constants of the

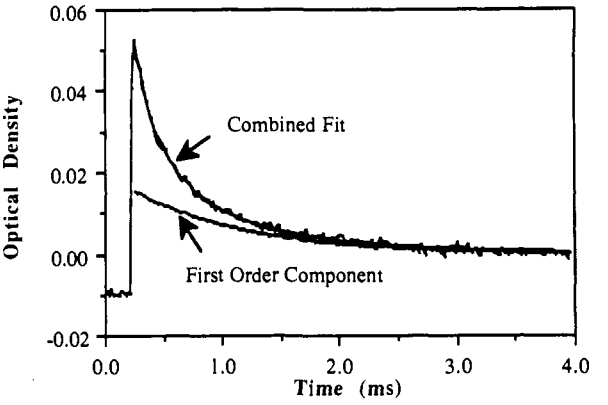

Figure 6. Transient decay observed (310 nm) following electron attachment to 2-(methoxymethyl)-1,4-benzoquinone (1.1×10^{-3} M) in N_2-saturated phosphate buffer solution at pH 3 containing 0.2 M *tert*-butyl alcohol (dose = 15 Gy/pulse). Solid lines include combined competing first- and second-order fit (upper) and its first-order component (lower).

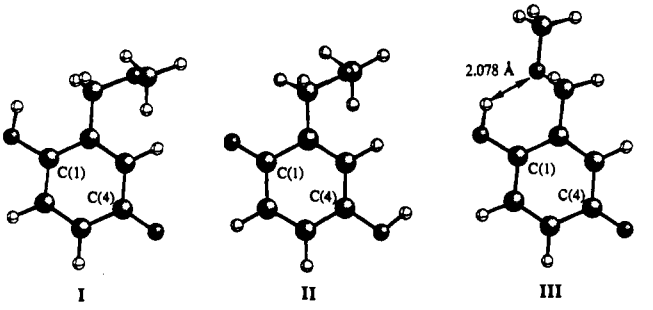

Figure 7. Optimized geometries for semiquinone of 2-(methoxymethyl)-1,4-benzoquinone. Conformer III suggests an intramolecular H-bonding of the phenolic hydrogen and the methoxy oxygen.

Table IV. Heats of Formation and C–X Bond Lengths for Different Semiquinone Radical Conformers[a]

	ΔH_f (kcal/mol), C–X (Å)		
quinone	I	II	III
1	−42.52, 1.932	−44.07, 1.933	
2	−55.32, 1.759	−56.37, 1.758	
3	−87.74, 1.418	−89.93, 1.421	−89.08, 1.429

[a] Conformations are illustrated in Figure 7.

methoxy and phenoxy adducts are similar, the first-order decay rate constant for the phenoxy model is 4 times larger than for the methoxy derivative, Table III. Attempts to fit these decays to a second-order process followed by a first-order process, which would be indicative of elimination from the hydroquinone, gave very marginal fits.

Calculations. Standard AM1 (UHF) procedure (see Experimental Section for details) was used to calculate spin distributions, formal charges, geometries, and heats of formation for the reduced bromo-, chloro-, and methoxy-α-methyl-substituted 1,4-benzoquinones. The bond lengths and angles of the semiquinones and semiquinone radical anions are almost identical, with the exception of the C–X bonds (X = Br, Cl, and OMe), in this series of compounds.

While protonation of the methoxy radical anion yields three conformers, Figure 7, the bromo and chloro adducts yield only two conformers (protonation at either oxygen). Although the heats of formation for the different conformers are within 2.0 kcal/mol, protonation of oxygen attached to C(4) leads to the most stable conformer for all the semiquinones studied. Protonation of oxygen attached to C(1) in the methoxy adduct yields two conformers, I and III, with the lower energy conformer, III, having a stabilizing interaction (H-bonding) between the phenolic hydrogen and the methoxy oxygen as is evidenced by the close proximity of the hydrogen and the methoxy oxygen (2.078 Å) and a slight

Scheme II. Proposed Mechanism for the pH-Dependent Decay of Singly Reduced α-Methyl Substituted 1,4-Benzoquinones

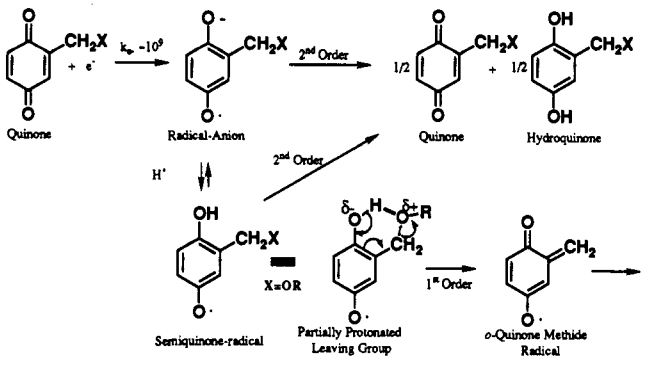

lengthening of the C–X bond, Table IV.

To study the effect of metals on the structure of the radical anion, a disembodied positive charge[22] was placed near the quinone oxygens. The resulting heats of formation for the semiquinone radical-anion "metal complex" suggest the metal complexation to the oxygen attached to C(1) and the methoxy oxygen is the most stable conformer. Spin distributions, formal charges, optimized geometries, and heats of formation for the reduced bromo-, chloro-, and methoxy-α-methyl-substituted 1,4-benzoquinones and the "metal complexes" are included in the supplementary material.

Discussion

Substituent and pH play an important role in the chemistry of pulse radiolytically reduced α-methyl-substituted 1,4-benzoquinones. The observed transient absorption spectra and decay kinetics of all the reduced models are similar at pH 7. The transient decay is second order, and the rate constants are unaffected over a range of doses and concentrations. The transient half-lives decrease with increasing dose, as is characteristic of a second-order process. Thus, at pH 7, the semiquinone radical anion disproportionates at virtually the same rate, irrespective of substituent, implying that the loss of the substituent is not kinetically competitive with disproportionation.

At pH 3, the transients formed from the bromo- and chloro-substituted models still exhibit simple second-order decay (by disproportionation), but the methoxy- and phenoxy-substituted 1,4-benzoquinones decay via competing first- and second-order processes, which can be reasonably assigned to *o*-quinone methide radical formation and disproportionation, respectively. The following mechanism is therefore proposed to account for the pH-dependent decay kinetics observed for *o*-quinone methide radical formation, Scheme II.

With electron attachment rates of $\sim 2 \times 10^9$ M^{-1} s^{-1}, the substituted quinones are reduced to form semiquinone radical anions, which disproportionate to give the quinone and the dianion of the hydroquinone at pH 7. At lower pH, the semiquinone radical anion is readily protonated, producing a semiquinone radical that disproportionates regardless of substituent (X = Br, Cl, and OR). In the methoxy- and phenoxy-substituted models, intramolecular hydrogen bonding of the phenolic OH to the alkoxy leaving group is also possible, yielding a much better leaving group and leading to more facile formation of the *o*-quinone methide radical. This mechanism can account for the different kinetics observed at pH 3 and 7. While the semiquinone radical anion at pH 7 disproportionates regardless of substituent, at lower pH it is readily protonated to the semiquinone radical, which can disproportionate or, in the methoxy- and phenoxy-substituted models, decay via proton-assisted elimination to an *o*-quinone methide radical in competition with the second-order disproportionation. Since the *o*-quinone methide radical is expected to be highly reactive and is formed in competition with disproportionation, it is not surprising that attempts to characterize it were unsuccessful. There is no evidence, in the form of spectral changes or decay kinetics, for elimination from the hydroquinone (or the dianion) of these models within 200 ms of the pulse.

Conclusions

The results of these studies provide evidence for reductive elimination from the singly reduced state of some α-methyl-substituted 1,4-benzoquinones at low pH. Electron attachment rates, absorption spectra, extinction coefficients, and pK_a's for the reduced quinones are very similar regardless of substituent, but the decay kinetics are dependent on both substituent and pH. The semiquinone radical anions at pH 7 disproportionate regardless of substituent, while at pH 3 the radical anion is readily protonated and the phenoxy- and methoxy-substituted models decay by competing first- and second-order processes, presumably indicative of reductive elimination becoming competitive with disproportionation. The involvement of an intramolecular H-bonded intermediate is proposed in the formation of the *o*-quinone methide radical. Calculations support the existence of such an intermediate. Metal chelation to form an analogous intermediate is energetically favored, thus raising the interesting question of the possible role of metal ions or intercellular acidity[27,36] in the activation of these drugs.[37]

Although these models vastly oversimplify the structures of active bioreductive alkylating agents, these quinone methide radicals can be envisaged as rising by a reductive elimination from appropriately substituted benzoquinones, naphthoquinones, anthraquinones, anthracyclines, and other related systems common to these drugs.[2] It may be possible to increase the activity and efficiency of the bioreductive alkylating agents by incorporating functionality that can act as an internal acid catalyst to facilitate elimination following reduction.[38] Electrochemical and ESR studies of these models and the analogous naphthoquinones are currently under way.

Acknowledgment. This work was supported by the National Institutes of Health (Grant No. RR00886). The pulse radiolysis experiments were conducted at the Center for Fast Kinetics Research, which is jointly supported by the National Institute of Health and the University of Texas. We thank Dr. R. B. Draper and B. K. Naumann for the assistance in the pulse radiolysis experiments and Yajun Zheng for his patience and help with the calculations.

Supplementary Material Available: Tables of the spin densities, formal charges, heats of formation, and optimized geometries calculated for the radical anions, semiquinone radicals, and the metal complexes (6 pages). Ordering information is given on any current masthead page.

(36) Kohn, H.; Hong, Y. P. *J. Am. Chem. Soc.* **1990**, *112*, 4596.
(37) Butler, J.; Hoey, B. M.; Swallow, A. J. *FEBS Lett.* **1985**, *182*, 95.
(38) Islam, I.; Skibo, E. B. *J. Org. Chem.* **1990**, *55*, 3195.